

From human mesenchymal stromal cells to osteosarcoma cells classification by deep learning

Mario D’Acunto^a, Massimo Martinelli^b and Davide Moroni^{b,*}

^a*Institute of Biophysics, National Research Council of Italy, Via Moruzzi, 1 – 56124-Pisa (IT)*

^b*Institute of Information Science and Technologies, National Research Council of Italy, Via Moruzzi, 1 – 56124-Pisa (IT)*

Abstract. Early diagnosis of cancer often allows for a more vast choice of therapy opportunities. After a cancer diagnosis, staging provides essential information about the extent of disease in the body and the expected response to a particular treatment. The leading importance of classifying cancer patients at the early stage into high or low-risk groups has led many research teams, both from the biomedical and bioinformatics field, to study the application of Deep Learning (DL) methods. The ability of DL to detect critical features from complex datasets is a significant achievement in early diagnosis and cell cancer progression. In this paper, we focus the attention on osteosarcoma. Osteosarcoma is one of the primary malignant bone tumors which usually afflicts people in adolescence. Our contribution to classification of osteosarcoma cells is made as follows: a DL approach is applied to discriminate human Mesenchymal Stromal Cells (MSCs) from osteosarcoma cells and to classify the different cell populations under investigation. Glass slides of different cell populations were cultured including MSCs, differentiated in healthy bone cells (osteoblasts) and osteosarcoma cells, both single cell populations or mixed. Images of such samples of isolated cells (single-type or mixed) are recorded with traditional optical microscopy. DL is then applied to identify and classify single cells. Proper data augmentation techniques and cross-fold validation are used to appreciate the capabilities of a convolutional neural network to address the cell detection and classification problem. Based on the results obtained on individual cells, and to the versatility and scalability of our DL approach, the next step will be its application to discriminate and classify healthy or cancer tissues to advance digital pathology.

Keywords: Human mesenchymal stromal cells, Osteosarcoma cells, deep learning, convolutional neural networks, convolutional object detection systems, cell classification

1. Introduction

Every year, several million people die of cancer in the world due to the inaccessibility of appropriate detection schemes and consequent ineffective treatments [17]. Over the last decades, scientists have

applied different methods to detect cancer tissues at an early stage. Such investigation is motivated by the fact that early diagnosis can facilitate the clinical management of patients. As a consequence, researchers have been examining methods for the early detection of cancers via several methods including cancer screening, solid, liquid and optical biopsy, prognostic determination, and monitoring. However, up till now, there are no known diagnostic procedures that do not hurt the physical health of patients during the process of cancer detection, being such

*Corresponding author. Davide Moroni, Institute of Information Science and Technologies, National Research Council of Italy, Via Moruzzi, 1 – 56124-Pisa (IT). E-mail: davide.moroni@isti.cnr.it.

a method invasive. Consequently, early diagnosis should require the ability not only to identify cancer tissue as small as a single cell but having non-invasiveness as a prerequisite.

Classification of cancer cells is hence essential research for early diagnosis and identification of differentiation and progression of cancer in a single cell [11, 21, 24].

With the advent of new digital technologies in the field of medicine, Artificial Intelligence (AI) methods have been applied in cancer research to complex datasets in order to discover and identify patterns and relationships between them. Machine Learning (ML) is a branch of AI related to the problem of learning from data samples to the general concept of inference. In turn, DL is a part of ML methods based on learning data representation. DL algorithms, in particular, convolutional networks, have rapidly become a methodology of choice for analyzing medical images. A fundamental concept in DL is to let computers learn the features that optimally represent the data for the problem to be handled. This goal can be approached by building models (networks) composed of many layers that transform input data (in our case medical images) to outputs (e.g. a classification such as disease being present/absent) while learning increasingly higher level features. In the last decade of application of DL to medical images, Convolutional Object Detection (COD) has become a successful approach to cancer analysis. In this paper, we have investigated the use of a COD-based method to several differentiated samples of cells cultured on a glass slide, with the purpose to discriminate osteosarcoma cells from MSCs (osteoblasts). The results are auspicious, exhibiting an accuracy of nearly one on the available dataset. These results related to the classification of cells of different malignant degree, ranging from normal to cancer cells, can generate important advantages in the study of cell seeding and cell growth. Indeed, such results allow efficient analysis of single cells simply by employing an optical microscope without using conventional biochemical methods that are time-consuming and may require a large number of cells. The next step will be to extend the algorithm to large populations of cells and tissues with the purpose to improve digital histopathology. The paper is organized as follows. First, related works are described in Section 2. Section 3 describes materials and methods, focusing on the procedure followed for the cell culture (3.1), on the construction, augmentation, and annotation of the dataset (3.2) and, finally, on the chosen network architecture (3.3).

Section 4 reports the results of the training and accuracy of the method applied. Finally, Section 5 concludes the paper with discussion for future work. This paper extends our conference contribution [7].

2. Related works

The automatic classification of biological samples has received a lot of attention during the last years. Most of the conventional approaches rely on a feature extraction step, followed by feature classification for detecting the presence of structures of interest in biological images. Traditional methods have been based on handcrafted features, mainly consisting in descriptors of shape and appearance, including color and texture features. In this approach, general-purpose and ad hoc features are computed on the region of interest or the segmented structure of interest to gather into a single vector all the information for solving the visual task. By contrast, in DL approaches, significant features for the visual task are not defined *a priori* but they are learned during the training process. Such a new approach has recently shown expert-level accuracy in medical image classification, improving new methods in diagnostic pathology [4]. Digital pathology exploits the quantification and classification of digitized tissue samples by supervised deep learning. This innovative approach to histopathology making use of digital methodologies has shown excellent results even for tasks previously considered too challenging to be accomplished with conventional image analysis methods [5, 8, 14, 18, 19, 29]. In histopathology, several DL results have recently appeared. In [16], the authors present two successful applications of DL in reducing the workload for pathologists, namely prostate cancer identification in biopsy specimens and breast cancer metastasis detection in sentinel lymph nodes. Their work proves the potential of DL in increasing objectivity of diagnoses; indeed all glass slides in which prostate cancer and micro- and macro-metastases of breast cancer were present were automatically detected; slides featuring normal tissue only could be excluded without the use of any additional immunohistochemical markers or human intervention. Similarly, in [30], a CNN is trained to provide a simple, efficient and effective method for achieving state-of-the-art classification and segmentation for the MICCAI 2014 Brain Tumor Digital Pathology Challenge. Transfer learning was used in their work, starting with a network pre-trained on an

141 extensive general image database. Again, in [9], the
142 authors address the classification of breast cancer his-
143 tology images using transfer learning starting with
144 the general Inception Resnet v2 for direct labeling of
145 the full images. In [3], the authors proposed two dif-
146 ferent CNN architectures for breast cancer, namely a
147 single task CNN is used to predict malignancy and
148 multi-task CNN is used to predict both malignancy
149 and image magnification level simultaneously. The
150 results of their methods are compared using as a
151 benchmark the BrecaKHis dataset. All the previous
152 works discussed above deal with general histological
153 images to classify the whole images in order to decide
154 whether there is or not the presence of malignant cells.
155 Concerning the specific case of osteosarcoma, which
156 is the focus of the present paper, in [20], a CNN is
157 defined, trained and evaluated on hematoxylin and
158 eosin stained images. The goal of their network is to
159 assign tumor classes (viable tumor, necrosis) versus
160 non-tumor directly to input slide images.

161 Also, many tasks in digital pathology, directly or
162 indirectly connected to tumor cell differentiation,
163 require the classification of small clusters of cells up
164 to a single cell, if possible. For this purpose, differ-
165 ently, from the works mentioned above, this paper
166 investigates the classification of single cultured cells
167 with a known grade of differentiation with a super-
168 vised DL approach. Specifically, COD-based DL
169 method is applied to several differentiated samples of
170 cells cultured on a glass slide, with the primary pur-
171 pose to discriminate osteosarcoma cells from MSCs
172 (osteoblasts).

173 Within the ML techniques applied for the analysis
174 of cancer cells, recently, COD has gained consider-
175 able interest [7]. Besides, several methods have been
176 proposed to address the object recognition task, and
177 many software frameworks have been implemented
178 to design, train and use deep learning networks (such
179 as Caffe [12], Apache MXNet [1] and many others).
180 Among all such methods, Google TensorFlow [2] is
181 currently one of the most used frameworks, and its
182 Object Detection API emerged as a potent tool for
183 image recognition. Since the case study proposed in
184 this paper requires the highest accuracy architecture
185 allowable, we selected the Faster Region Convolu-
186 tional Neural Network (Faster R-CNN) [22, 23] that
187 is an original region proposal network sharing fea-
188 tures with the detection network that improves both
189 region proposal quality and object detection accuracy.
190 Faster R-CNN uses two networks: a Region Proposal
191 Network (RPN) to generate region proposals and a
192 detector network to discover object instances. The

193 RPN produces region proposals more quickly than
194 the Selective Search [27] algorithm used in previ-
195 ous solutions. By sharing information between the
196 two networks, the accuracy is also improved, and this
197 solution is currently the one with the best results in the
198 latest object detection competitions. Faster R-CNN
199 approach can be applied using several network archi-
200 tecture as elemental deep features encoders. In [10]
201 a guide for selecting the right architecture depending
202 on speed, memory and accuracy is provided.

203 Concerning general purpose CODs, evaluating a
204 DL approach to digital histopathology poses the
205 problem of collecting a dataset sufficiently rich for
206 performing an adequate training of the network.
207 Indeed, as it is well known, DL methods require
208 many examples to understand and learn the best rep-
209 resentation of an object model. Some of the works
210 as mentioned above resorted to the use of transfer
211 learning, starting with a network pre-trained on large
212 datasets, such as ImageNet. However, also proper
213 data augmentation strategies have been used with
214 good results to overcome over-fitting issues. Con-
215 ventional data augmentation methods address both
216 the spatial and appearance domains of the images, by
217 applying to the original images geometrical transfor-
218 mations (mainly orthogonal transformation such as
219 rotations and mirroring) and/or intensity transforma-
220 tions (e.g. contrast stretching). For instance, in [13],
221 the authors use spatial data augmentation (arbitrary
222 rotation, mirroring and scaling) during the training
223 of all models, while noticing that the most prominent
224 source of variability in histopathology images is the
225 staining color appearance. In [28], they propose a so-
226 called multi-scale fusion data augmentation method:
227 their original database is augmented with a factor of
228 14 by rotation, scaling and mirroring randomly over
229 all samples. They employed rotations by multiples of
230 the right angle and a scale factor up to 0.8, as well
231 as horizontal and vertical mirroring, addressing the
232 classification problem of breast cancer pathological
233 images.

234 3. Material and methods

235 3.1. Cells Culture

236 Normal, cancerous and mixed cells were cultured
237 on glass slides. Details can be found in [7]; in
238 this paper we briefly describe the essential differ-
239 ence among the cell populations under investigation.
240 Undifferentiated MSCs were isolated from human

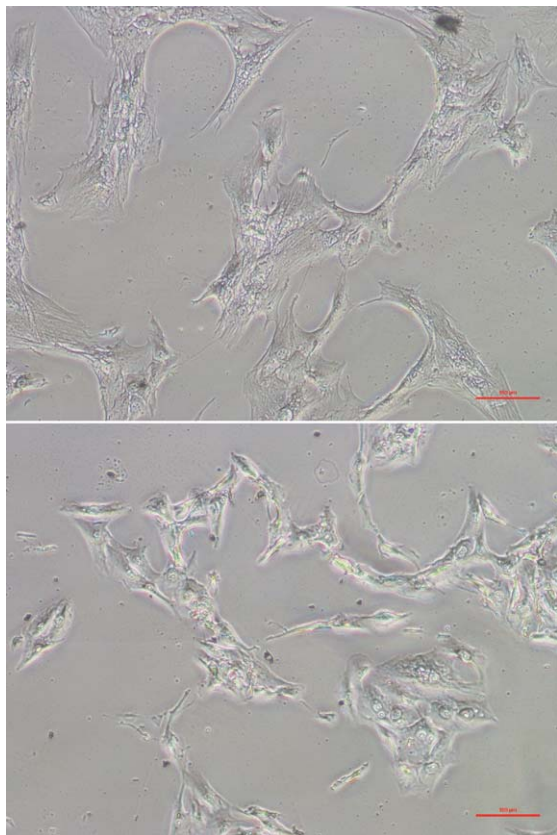


Fig. 1. Morphology of osteoblast cells, (top, 10× objective, scale bar 100µm), and osteosarcoma cells (bottom, 10× objective, scale bar 100µm).

bone marrow according to a previously reported method [25] and used to perform three culture strategies. MSCs were plated on glass slides inside Petri dishes at a density of 20,000 cells with 10% fetal bovine serum (FBS). The samples were cultured for 72 h, then fixed in 1% neutral buffered formalin for 10 min at 4°C. Osteosarcoma cells consisted of human cells, named MG-63, were seeded on six glass slides at 10,000 cells. Finally mixed cancer and healthy cells were plated on six glass slides inside Petri dishes at 10,000 cells with 10% FBS.

At each endpoint, all the samples were fixed in 1% (w/v) neutral buffered formalin for 10min at 4°C. Morphologies are visible in Figure 1, as imaged by an inverted microscope (Nikon Eclipse Ti-E).

3.2. Data set collection, annotation and augmentation

A total of $N = 60$ images has been collected using two different microscopes, working in two different

color spaces: one acquires conventional RGB images while the other acquires monochrome images with green background density. Experienced users have manually annotated all the images. Namely, it was requested to identify in each of the images a number of rectangular regions corresponding to particular cells and cell clusters. Five categories have been used to label the regions:

- a) Single cancer cell
- b) Cancer cluster
- c) Single MSC cell
- d) MSC cluster
- e) Artifact

To ease the annotation tasks, a graphical interface for performing annotation has been provided to the experts. The interface is based on the Labelling Software [26] and allows to insert multiple instances of labeled regions in each of the images in the dataset. A total of 279 objects were labeled in the images.

The dataset was therefore augmented applying both spatial and intensity transformations. With respect to other approaches that perform augmentation online directly during the training stage by applying transformations randomly, in this paper augmentation was performed offline before training. Since the dataset contains a relatively small number of images and objects when compared to large general image datasets, there is no memory and efficiency concern in the present case. For spatial transformations, we applied the dihedral group D_4 consisting of the symmetries of the square. Each image and the associated labeled regions were transformed accordingly, yielding a $\times 8$ boost in the number of samples in the dataset. As for what regards the color space, power law transform has been used to augment the datasets and make the results more robust with respect to illumination changes:

$$O = C \cdot \gamma^i$$

where i represents the original input pixel value, O is the output pixel value obtained after power law transformation and C, γ are the parameters of the transform. In our experiments, we fixed $C = 1$ and $\gamma = 3/4, 4/5, 1, 5/4, 4/3$. In the case of RGB images, the power law transform was applied to each color channel. In general, such a procedure allowed for a $\times 5$ boost in dataset size.

Finally, images and labels were automatically converted into the relative TensorFlow formats. Images were encoded into TensorFlow records, and labels

290 were produced into Comma Separated Values (CSV)
 291 listing. Each row in the CSV listing contains the file-
 292 name, the image size, the label and the top-left and
 293 bottom-right corner of the object determined by the
 294 domain expert.

295 3.3. CNN for cell detection and classification

296 Among the possible approaches to COD, in this
 297 paper, Faster R-CNN is adopted. Faster R-CNN uses
 298 two sub-networks: a deep fully convolutional net-
 299 work that proposes regions (named Region Proposal
 300 Network - RPN) and another module that classifies
 301 the proposed regions (classification network) [22].
 302 The two sub-networks share the first layers which
 303 act as a feature extraction module. Several architec-
 304 tures can be used for building the feature extraction
 305 module. Specifically, Inception Resnet v2 model was
 306 selected in this paper and instantiated for this par-
 307 ticular application making use of TensorFlow [2].
 308 Transfer learning was used to cope with the limited
 309 dataset of images, which is not sufficient for deal-
 310 ing with training from scratch. Namely, an inference

311 graph for Inception Resnet v2 pre-trained on COCO
 312 dataset [15] has been imported. On the basis of the
 313 feature extracted, the RPN produces candidates for
 314 regions that might contain objects of interest. Namely,
 315 sliding a small window on the feature map, the RPN
 316 produces probabilities about the object presence in
 317 that region for region boxes of fixed aspect ratio and
 318 scale; a bounding box regressor also provides opti-
 319 mal size and position of the candidate rectangular
 320 areas in an intrinsic coordinate system. Candidates
 321 with a high probability of object presence are then
 322 passed to the classification network that is in charge
 323 of assessing the presence of an object category inside
 324 the region. As a training strategy, firstly only the final
 325 fully connected layers of the two sub-networks were
 326 trained, leaving frozen all the other layers. In a fine-
 327 tuning phase, also the layers in the feature extraction
 328 module were optimized by using the training routines
 329 made available in TensorFlow.

330 4. Results

331 Given the limited dataset available and with the
 332 primary goal of demonstrating the applicability of
 333

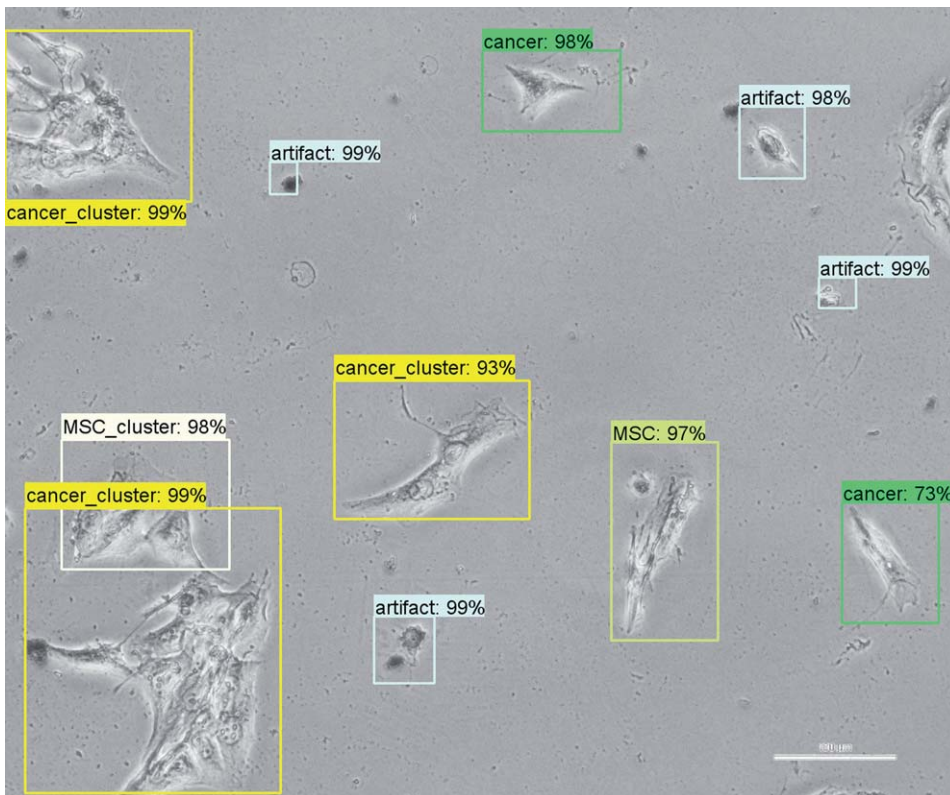


Fig. 2. An example of RGB image with localized and recognized objects. Examples from the all 5 classes described in Section 3.2 are shown.

DL to the problem of cell classification, it was opted to perform n -fold cross validation with $n = 5$ in order to obtain more statistically significant results. The original set A of $N = 60$ images was partitioned into $n = 5$ non-overlapping subsets A_1, A_2, \dots, A_5 with 12 images each. The data augmentation strategy described in Section 3.2 was then applied to each subset A_i ($1 \leq i \leq 5$) producing the extended set \bar{A}_i with cardinality $\#\bar{A}_i = 480$ as well an associated list of labeled regions.

Multiple training and validation sessions were then carried out. In particular for each j ($1 \leq j \leq 5$), a network \mathcal{N}_j was optimized using as training set $B_j = \bigcup_{i \neq j} \bar{A}_i$, while the set \bar{A}_j might be used for validation. Notice that we opted for this partitioning approach in order to keep fully separated the training set from the validation set. Approximately, the proportion of the split between training and validation is 4 : 1, since the number of regions of interest contained in each subset \bar{A}_j does not vary significantly.

As an additional experiment, the same training procedure was repeated not taking in input the original monochrome and RGB images, but converting first all the the images to grayscale using [6].

Each training phase lasted five days for all the training sets, using 300 regions proposals and learning parameters set to 10^{-4} for the first 90.000 cycle and then reduced to 10^{-5} . In the RPN, four scales corresponding to 1/4, 1/2, 1, 2 and three aspect ratios 1/2, 1, 2 were used.

All the inference graphs produced have been exported and tested for inference on the validation set.

Figure 2 reports examples of localization and recognition using the first graph on a RGB image. Figure 3 shows an example of the second graph localization and recognition on another gray-scale image.

The average accuracy obtained using RGB and the original monochrome images was 0.975 ± 0.01 . When using the images converted to grayscale very

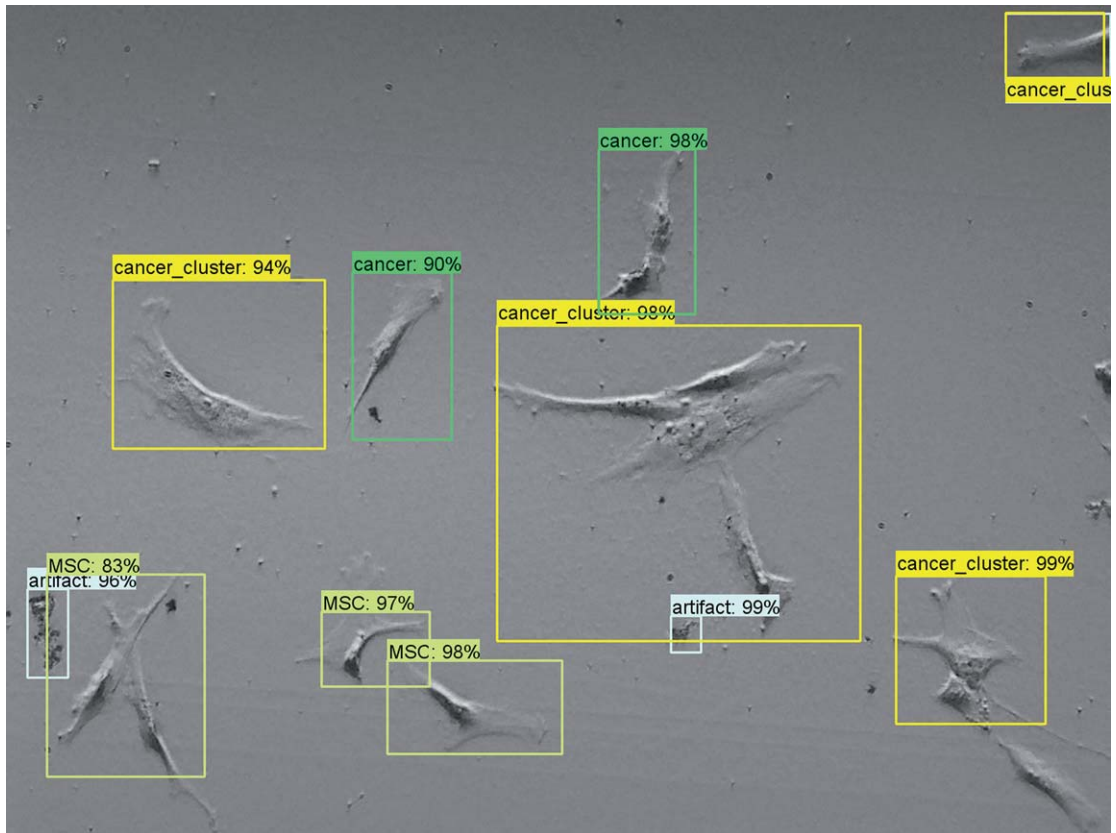


Fig. 3. An example of gray-scale image with localized and recognized objects under investigation. In this case, example from all the classes reported in Section 3.2 but MSC.cluster are shown.

similar results have been found with an accuracy of 0.972 ± 0.005 .

On the basis of these results, the use of color seems not to provide significant information for classification.

All training procedures have been executed on a PC with a 4 cores 8 threads Intel(R) Core(TM) i7-4770 CPU @ 3.40 featuring 16 Giga Bytes DDR3 of RAM, an Nvidia Titan X powered with Pascal, and Ubuntu 16.04 as operating system. Localization and recognition of new images require less than one second on a personal computer with a modern Intel I7 CPU.

5. Conclusions

Classification of single or small clusters of cancer cells is a crucial question for early diagnosis. In this paper, a Deep Learning approach to recognize single or small clusters of cancer cells has been presented. The Deep Learning method adopted was based on Faster-RCNN technique and applied to several samples of cells cultured on glass slide with the purpose to discriminate osteosarcoma cells from osteo-differentiated MCSs (osteoblasts). The ability of such an algorithm to identify and classify approximately the 100% of the investigated cells potentially will allow us to extend the method to large population cells or tissues. These results related to the classification of cells of different malignant degree, ranging from normal to cancer cells, can have significant consequences in the study of cell seeding and cell growth. Another essential advantage of our results is that they allow efficient analysis of single cells by merely employing an optical microscope without using conventional biochemical methods that are time-consuming and may require a large number of cells. The next step will be to extend the algorithm to large populations of cells and tissues with the purpose to improve digital histopathology.

Acknowledgements

This research was performed in the framework of the BIO-ICT lab, a joint initiative by the Institute of Biophysics (IBF) and the Institute of Information Science and Technologies (ISTI), both of the National Research Council of Italy (CNR).

We would like to thank NVIDIA Corporation for its support: this work would have been very time-consuming without a Titan X board powered by

Pascal that was granted by NVIDIA to the Signals & Images Lab of ISTI-CNR in 2017.

In turn, we wish to thank Serena Danti, from the Department of Engineering, University of Pisa, and Luisa Trombi and Delfo D'Alessandro, from the Department of Medicine, University of Pisa, for useful support with biological samples.

References

- [1] <https://mxnet.apache.org/>. <https://mxnet.apache.org/>, 2019. Last retrieved May 3, 2019.
- [2] M. Abadi, P. Barham, J. Chen, Z. Chen, A. Davis, J. Dean, M. Devin, S. Ghemawat, G. Irving, M. Isard, et al., TensorFlow: A system for large-scale machine learning, *In 12th USENIX Symposium on Operating Systems Design and Implementation (OSDI 16)*, 2016, pp. 265–283.
- [3] N. Bayramoglu, J. Kannala and J. Heikkilä, Deep learning for magnification independent breast cancer histopathology image classification, *In 2016 23rd International Conference on Pattern Recognition (ICPR)*, IEEE, 2016, pp. 2440–2445.
- [4] D. Bychkov, N. Linder, R. Turkki, S. Nordling, P.E. Kovanen, C. Verrill, M. Walliander, M. Lundin, H. Caj and J. Lundin, Deep learning based tissue analysis predicts outcome in clorectal cancer, *Scientific Reports* **8** (2018).
- [5] D.C. Cireşan, A. Giusti, L.M. Gambardella and J. Schmidhuber, Mitosis detection in breast cancer histology images with deep neural networks, *In International Conference on Medical Image Computing and Computer-assisted Intervention*, Springer, 2013, pp. 411–418.
- [6] J. Cristy, Imagemagick website, 2013. Accessed 2018-10-30.
- [7] M. D'Acunto, M. Martinelli and D. Moroni, Deep learning approach to human osteosarcoma cell detection and classification, *In International Conference on Multimedia and Network Information System*, Springer, 2018, pp. 353–361.
- [8] O. Dürr and B. Sick, Single-cell phenotype classification using deep convolutional neural networks, *Journal of Biomolecular Screening* **21**(9) (2016), 998–1003.
- [9] C.A. Ferreira, T. Melo, P. Sousa, M.I. Meyer, E. Shakibapour, P. Costa and A. Campilho, Classification of breast cancer histology images through transfer learning using a pre-trained inception resnet v2, *In International Conference Image Analysis and Recognition*, Springer, 2018, pp. 763–770.
- [10] J. Huang, V. Rathod, C. Sun, M. Zhu, A. Korattikara, A. Fathi, I. Fischer, Z. Wojna, Y. Song, S. Guadarrama and K. Murphy, Speed/accuracy trade-offs for modern convolutional object detectors, *In 2017 IEEE Conference on Computer Vision and Pattern Recognition, CVPR 2017, Honolulu, HI, USA, 2017*, pp. 3296–3297.
- [11] H.A. Idikio, Human cancer classification: A systems biology-based model integrating morphology, cancer stem cells, proteomics, and genomics, *Journal of Cancer* **2** (2011).
- [12] Y. Jia, E. Shelhamer, J. Donahue, S. Karayev, J. Long, R. Girshick, S. Guadarrama and T. Darrell, Caffe: Convolutional architecture for fast feature embedding, *In Proceedings of the 22nd ACM International Conference on Multimedia*, ACM, 2014, pp. 675–678.

- 479 [13] M.W. Lafarge, J.P.W. Pluim, K.A.J. Eppenhof, P. Moeskops
480 and M. Veta, Domain-adversarial neural networks to address
481 the appearance variability of histopathology images, In
482 *Deep Learning in Medical Image Analysis and Multimodal*
483 *Learning for Clinical Decision Support*, Springer, 2017,
484 pp. 83–91.
- 485 [14] Z. Li, S.M.R. Soroushmehr, Y. Hua, M. Mao, Y. Qiu and K.
486 Najarian, Classifying osteosarcoma patients using machine
487 learning approaches, In *2017 39th Annual International*
488 *Conference of the IEEE Engineering in Medicine and Biol-*
489 *ogy Society (EMBC)*, 2017, pp. 82–85.
- 490 [15] T.-Y. Lin, M. Maire, S. Belongie, J. Hays, P. Perona,
491 D. Ramanan, P. Dollár and C.L. Zitnick, Microsoft coco:
492 Common objects in context, In *European Conference on*
493 *Computer Vision*, Springer, 2014, pp. 740–755.
- 494 [16] G. Litjens, C.I. Sánchez, N. Timofeeva, M. Hermsen, I.
495 Nagtegaal, I. Kovacs, C.H.-V. De Kaa, P. Bult, B.V. Gin-
496 ncken and L.J. Van Der, Deep learning as a tool for increased
497 accuracy and efficiency of histopathological diagnosis, *Sci-*
498 *entific Reports* **6** (2016), 26286.
- 499 [17] S. McGuire, World cancer report 2014, Geneva, Switzer-
500 land: World Health Organization, international agency for
501 research on cancer, WHO Press, 2015, 2016.
- 502 [18] R. Mishra, O. Daescu, P. Leavey, D. Rakheja and A. Sen-
503 gupta, Convolutional neural network for histopathological
504 analysis of osteosarcoma, **25**(10) 2017.
- 505 [19] R. Mishra, O. Daescu, P. Leavey, D. Rakheja and A.
506 Sengupta, Histopathological diagnosis for viable and
507 non-viable tumor prediction for osteosarcoma using con-
508 volutional neural network, In Z. Cai, O. Daescu and M. Li,
509 editors, *Bioinformatics Research and Applications*, Cham,
510 Springer International Publishing, 2017, pp. 12–23.
- 511 [20] R. Mishra, O. Daescu, P. Leavey, D. Rakheja and A.
512 Sengupta, Histopathological diagnosis for viable and
513 non-viable tumor prediction for osteosarcoma using con-
514 volutional neural network, In *International Symposium on*
515 *Bioinformatics Research and Applications*, Springer, 2017,
516 pp. 12–23.
- 517 [21] A.A. Nahid, M.A. Mehrabi and K. Yanan, Histopathological
518 breast cancer image classification by deep neural network
519 techniques guided by local clustering, *BioMed Research*
520 *International* **2018** (2018).
- [22] S. Ren, K. He, R. Girshick and J. Sun, Faster r-cnn: Towards
521 real-time object detection with region proposal networks. In
522 C. Cortes, N.D. Lawrence, D.D. Lee, M. Sugiyama and R.
523 Garnett, editors, *Advances in Neural Information Process-*
524 *ing Systems* **28**, Curran Associates, Inc., 2015, pp. 91–99.
- [23] S. Ren, K. He, R. Girshick and J. Sun, Faster r-cnn: Towards
525 real-time object detection with region proposal networks,
526 *IEEE Transactions on Pattern Analysis and Machine Intel-*
527 *ligence* **39**(6) (2017), 1137–1149.
- [24] Q. Song, S.D. Merajver and J.Z. Li, Cancer classification
528 in the genomic era: Five contemporary problems, *Human*
529 *Genomics* **9** (2015).
- [25] L. Trombi, L. Mattii, S. Pacini, D. D'Alessandro, B. Bat-
530 tolla, E. Orciuolo, G. Buda, R. Fazzi, S. Galimberti and M.
531 Petrini, Human autologous plasma-derived clot as a biolog-
532 ical scaffold for mesenchymal stem cells in treatment of
533 orthopedic healing, *Journal of Orthopaedic Research* **26**(2)
534 (2008), 176–183.
- [26] Tzatalin. Labelimg. git code. <https://github.com/tzatalin/labelImg>,
535 2015. Last accessed 11 May 2018.
- [27] J.R.R. Uijlings, K.E.A. van de Sande, T. Gevers and A.W.M.
536 Smeulders, Selective search for object recognition, *Intern-*
537 *ational Journal of Computer Vision* (2013).
- [28] B. Wei, Z. Han, X. He and Y. Yin, Deep learning model
538 based breast cancer histopathological image classification.
539 In *2017 IEEE 2nd International Conference on Cloud Com-*
540 *puting and Big Data Analysis (ICCCBDA)*, IEEE, 2017,
541 pp. 348–353.
- [29] Y. Xie, F. Xing, X. Kong, H. Su and L. Yang, Beyond classi-
542 fication: Structured regression for robust cell detection using
543 convolutional neural network, In *International Conference*
544 *on Medical Image Computing and Computer-Assisted Inter-*
545 *vention*, Springer, 2015, pp. 358–365.
- [30] Y. Xu, Z. Jia, Y. Ai, F. Zhang, M. Lai, I. Eric and C.
546 Chang, Deep convolutional activation features for large
547 scale brain tumor histopathology image classification and
548 segmentation, In *2015 IEEE International Conference on*
549 *Acoustics, Speech and Signal Processing (ICASSP)*, IEEE,
550 2015, pp. 947–951.

Preprint